Journal of the Korean Society of Surveying, Geodesy, Photogrammetry and Cartography
Vol. 38, No. 2, 97-107, 2020
https://doi.org/10.7848/ksgpc.2020.38.2.97

ISSN 1598-4850(Print)
ISSN 2288-260X(Online)
Original article

Improvement of Vegetation Index Image Simulations by Applying Accumulated Temperature

Park, Jin Sue[1] · Park, Wan Yong[2] · Eo, Yang Dam[3]

Abstract

To analyze temporal and spatial changes in vegetation, it is necessary to determine the associated continuous distribution and conduct growth observations using time series data. For this purpose, the normalized difference vegetation index, which is calculated from optical images, is employed. However, acquiring images under cloud cover and rainfall conditions is challenging; therefore, time series data may often be unavailable. To address this issue, La *et al*. (2015) developed a multilinear simulation method to generate missing images on the target date using the obtained images. This method was applied to a small simulation area, and it employed a simple analysis of variables with lower constraints on the simulation conditions (where the environmental characteristics at the moment of image capture are considered as the variables). In contrast, the present study employs variables that reflect the growth characteristics of vegetation in a greater simulation area, and the results are compared with those of the existing simulation method. By applying the accumulated temperature, the average coefficient of determination (R^2) and RMSE (Root Mean-Squared Error) increased and decreased by 0.0850 and 0.0249, respectively. Moreover, when data were unavailable for the same season, R^2 and RMSE increased and decreased by 0.2421 and 0.1289, respectively.

Keywords : Image Simulation, Vegetation Index, Growth Characteristics, Accumulated Temperature

1. Introduction

Vegetation converts solar energy into chemical energy and it is the most important component of an ecosystem (Arnon *et al*., 1956). Changes in vegetation interact directly and indirectly with energy cycles, climate change, and human activities (Corenblit and Steiger, 2009). Therefore, vegetation distribution and growth analysis are essential for predicting changes in the environmental characteristics of the atmosphere, hydrology, and soil. (Boussetta *et al*., 2013).

Analyzing the temporal and spatial changes in vegetation requires the continuous observation of these changes using time series data (Lanorte *et al*., 2014). Vegetation indices are used to monitor the distribution, growth, and vitality of vegetation; among the various vegetation indices, the NDVI (Normalized Difference Vegetation Index) is commonly employed (Jensen, 2009). The NDVI is calculated via optical imaging through remote sensing, and various satellite images are used to observe the widely distributed vegetation (Pettorelli *et al*., 2005). Among these, LANDSAT, a multispectral satellite, has been in operation for more than 40 years and is suitable for constructing long-term time series NDVI data as it photographs in the infrared and visible bands (Robinson *et al*., 2017). However, in some cases, optical

Received 2020. 03. 03, Revised 2020. 03. 27, Accepted 2020. 04. 23
1) Member, Staff, ALLforLAND.Co.Ltd, Dept. of Advanced Technology Fusion, Konkuk University, (E-mail: mofeste@all4land.com)
2) Senior Principal Researcher, Agency for Defense Development (E-mail: wypark@add.re.kr)
3) Corresponding Author, Member, Professor, Dept. of Advanced Technology Fusion, Konkuk University (E-mail: eoandrew@konkuk.ac.kr)

images cannot be obtained owing to weather conditions, such as the presence of clouds and rainfall (Li and Yeh, 2004).

To overcome this problem, a method that uses images from various sensors has been suggested; however, data discontinuity occurs owing to the differences in sensor characteristics, such as the spatial and spectral resolutions between images (Jensen, 2009). An alternative method can produce a simulated image using acquired images. For this, the weighted average method (Lee *et al*., 2017) and the spatial and temporal adaptive reflectance fusion model (STARFM; Gao *et al*., 2006) have been employed with LANDSAT images. The weighted average method averages two images, one taken before and one after the target date, based on the date interval. The STARFM (Spatial and Temporal Adaptive Reflectance Fusion Model) fuses the characteristics of LANDSAT spatial resolution and MODIS (MOderate Resolution Imaging Spectroradiometer) temporal resolution, and result can be obtained even if only one LANDSAT image is captured 30 days before or after the target date. However, the conditions of the image vary depending on the season and region, and the images must be obtained from both the fusion sensors (Lee *et al*., 2017). The above two methods have limitations in that they cannot be employed if contiguous images are missing. The rainy season occurs in the Korean Peninsula during summer, and rain falls for an average of 103.5 days (data.kma.go.kr). Therefore, as LANDSAT has a 16-day revisit cycle, continuous data losses occur.

To address the limitations caused by the lack of simulation images obtained (when images at adjacent times are missing due to a continuous lack of data), a simulation method using multiple time images was proposed by La *et al*., (2015). This method utilizes accumulated LANDSAT data over a long period, and analyzes the relationship between an image and the variables of the period, and then it simulates an image for the target period. By using this method, an image for a desired target date can be simulated based on the acquired data, regardless of the acquisition cycle of the image. In the present study, we selected variables for use in the simulation that are related to the growth characteristics of vegetation and applied them to a wide area simulation to improve the simulation method proposed by La *et al*., (2015).

By producing a wide range of simulated images over a long period of omissions, it is expected that data from the Korean Peninsula can be used to construct a time series of vegetation index data for the Korean Peninsula, where rainfall is frequent during summer months and forests account for 63% of the land. Additionally, this method is expected to enable the determination of long-term forest distribution, as well as the analysis of growth and change forecasts. It is also expected to provide a measurement of the recovery criterion, and the simulated data can be employed to suggest directions that need to be taken with respect to forest loss due to disasters (such as forest fires on the east coast in 2000 and in Gangneung in 2019). Furthermore, it is expected to facilitate the identification of forest conditions in North Korea, in areas where access is limited, and to provide basic data for national development within the Korean Peninsula.

2. Methodology

2.1 La's method

La's method is a linear regression model that analyzes the relationship between long-term accumulated LANDSAT images and variables recorded on each image acquisition day (Eq. (1)) via the following:

$$Y^t_{(i,j)} = a_{1(i,j)}x^t_1 + a_{2(i,j)}x^t_2 + \cdots + a_{n(i,j)}x^t_n \quad (1)$$

where Y is the pixel value of a LANDSAT image, t is the target date, i and j a line and a column, respectively, $a_1 \ldots a_n$ are regression coefficients, and $x^t_1 \ldots x^t_n$ are the temperature, humidity, precipitation, visibility, reference NDVI, direct radiation, diffuse radiation, and reflected radiation occurring on the target date (Fig. 1 and Table 1).

The variables used are obtained from open data sources that are easily accessible, and temperature, humidity, precipitation, and visibility are obtained from the Korea Meteorological Administration.

The regression equation is calculated for each image pixel and a simulation is conducted. The variable applied to each pixel uses the same value without interpolation.

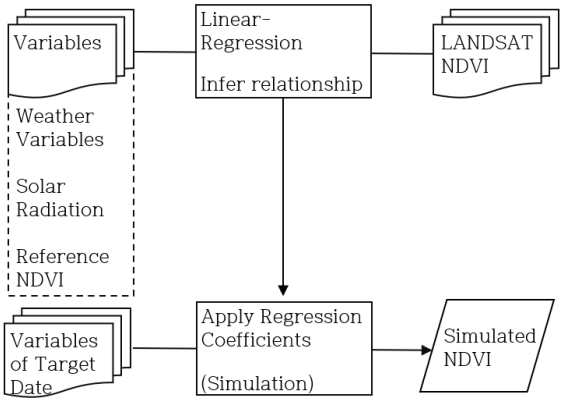

Fig. 1. Simulation process

Table 1. Variables used in La's method

Group	Variables
Weather variables	Temperature, Humidity, Precipitation, Visibility
Solar Radiation	Direct Radiation, Diffuse Radiation, Reflected Radiation
Vegetation Index	reference NDVI

The values of temperature, humidity, and visibility are those occurring at the time when the LANDSAT image would have been acquired, and precipitation is the daily average of that recorded from five days before image acquisition. The three solar radiation values employed are direct radiation, diffuse radiation, and reflected radiation, and the calculation method employs a DEM (Digital Elevation Model) in La's study (Kumar *et al*., 1997; Gates, 2012; La *et al*., 2015). In La's experiment, the ASTER GDEM (Advanced Spaceborne Thermal Emission and Reflection Radiometer Global DEM) was used; however, in this experiment, the SRTM (Shuttle Radar Topography Mission) DEM, which is known to have a higher vertical accuracy than ASTER GDEM, is employed (Hirt *et al*., 2010; Frey and Paul, 2012).

The reference NDVI value used in La's experiment was calculated from the LANDSAT image adjacent to the target date to be simulated.

La's image simulation method is easy to use, and its conditions are not demanding; therefore it has been compared with several other simulation methods (Lee *et al*., 2017; Kim *et al*., 2019). However, the process of selecting and processing the variables in La's method has not be improved, and no further research has been conducted.

2.2 Improvement direction

In La's experiment, to simulate the LANDSAT image, the reference NDVI calculated from other LANDSAT images of the adjacent period of the simulation target was used as a variable; however, the conditions (such as the range of the adjacent time) were not specified. Furthermore, NDVI cannot be calculated from LANDSAT images in adjacent periods when consecutive images are missing. Moreover, the problem about missing consecutive images is the limitation of the weighted average method (Lee *et al*., 2017) and STARFM method (Gao *et al*., 2006), The purpose of La's method is to address this limitation. It is a contradiction that La's method employed to solve the problem of lack of continuous images does not take into account the problem of obtaining a continuous image.

In this experiment, the MODIS NDVI image was resampled to 30m and used as an alternative reference NDVI variable. MODIS NDVI uses the vegetation index image MOD13Q1 provided by the Land Processes Distributed Active Archive Center (LP DAAC). MOD13Q1 has a spatial resolution of 250m, which is lower than that of LANDSAT, but the image is produced by processing values of 16 days, including the simulation target date. Thus, it can be used to provide the approximate NDVI condition of the target date.

The temperature, humidity, and visibility variables were used at the moment the image was acquired. It is possible to reflect the environment at the moment the image was acquired; however, the main change in the time series data is the vegetation, which grows with gradual changes in the weather. Weather variables that reflect the growth characteristics of vegetation, are discussed in detail in Section 2.3.

The experimental area employed in La's method was 24 × 24 km (576 km^2), which was less than 2% of the LANDSAT (185 × 185 km) image, and observations from two stations near the test area were used as variables. Although the simulation was proceeded for each pixel of the image, the variables used were applied without interpolation. In addition, the average values obtained at the two stations were applied equally to all pixels. In this study, the simulation

area is enlarged, and values from 18 stations are used. With an expansion of the simulation area, the values of weather variables are applied to each pixel using spline interpolation. This process is further described in Section 2.4.

2.3 Weather variable selection

La's method simulates missing image when the optical image cannot be obtained due to poor visibility during cloud cover, rainfall, and at high humidity and temperatures. If variables during cloudy and rainy conditions are applied to the relational formula built on the variables of the day when the ground image can be obtained, the simulation results may be inaccurate. To compensate for this, we aimed to apply the change in meteorological environment between acquisition days, rather than the using values on the acquisition day.

The NDVI provides data related to the observations of the vitality and distribution of vegetation during growth. Therefore, modeling should not employ the instantaneous environment at the time of imaging, but it should also consider gradual changes in the environment (Hänninen and Tanino, 2011). Vegetation grows and adapts to changes in climatic conditions such as temperature, humidity, and sunshine hours (Fenner, 1998). Among these variables, accumulated temperature, including temperature and time notion, is used to predict and observe vegetation growth stages (including flowering and foliation periods) (McMaster and Wilhelm, 1997). Depending on the species of vegetation and the purpose of the observations, different temperatures can be employed for various criteria (Kim *et al*., 2014). However, the minimum activation temperature of most vegetation is considered to be 0–5 ℃, and only values above that temperature are accumulated (Monteith, 1981).

To establish a standard for calculating accumulated temperature and cumulative precipitation, we analyzed the relationship between weather variables and NDVI images under various conditions.

To determine the relative importance of weather variables to the NDVI, the RF (Random Forest) (an ensemble learning method) (Breiman, 2001) was used to conduct a variable selection test. RF is type of machine learning that uses a combination of decision trees. Large data that are not sampled are divided into multiple training datasets through random sampling, and each dataset is trained through each decision tree. Combining multiple randomly generated decision trees can prevent overfitting and reduce the effects of noise. RF can be used to determine the importance of variables with respect to a regression problem (Breiman, 2001; Seo *et al*., 2017). The relative importance of NDVI and 16 weather variables was confirmed.

The test conducted on the selection of weather variables used 23 NDVI images captured on different dates, and 250,000 pixels of each image were analyzed.

However, for image simulation of the North Korean region, only weather records taken every 3 h were used (they were acquired in the same manner as North Korean weather data(data.kma.go.kr)).

The temperature at the time of acquisition used in La's study, average temperature, and accumulated temperature were compared. The average and accumulated values were calculated every 3 h, and the accumulation reference temperature was set to 0 ℃. The average temperature and accumulated temperature may be different due to the sub-zero temperature, so they were compared. To determine the difference according to the accumulated or average number of days, values from 4, 8, 12, and 16 days before the image was acquired were employed.

In addition to conducting this variable test, in the actual image simulation, there were no clouds and precipitation does not occur, on the day when images can be acquired. Therefore, precipitation was also compared to determine whether it should be employed as a weather variable. Precipitation has no negative value, and only average precipitation was used because the values of the mean and totalizer are the same (Table 2). Humidity and visible distance employed in La's method were excluded because they were not considered to be weather variables that directly affect the growth characteristics of vegetation; therefore, they are not related to the aim of this study.

The relative importance was calculated by analyzing the relationships between 5 million NDVI pixels and 16 variables (Fig. 2).

Table 2. Test weather variables

Type of Variables	Variables
Temperature	Temperature at the time when the image was acquired (T-img) Accumulated temperature and average temperature on the day of image acquisition (T-M1, T-A1) Average temperature over 4, 8, 12 and 16 days (T-M4, T-M8, T-M12, T-M16) Accumulated temperature over 4, 8, 12 and 16 days (T-M4, T-M8, T-M12, T-M16) (above 0 ˚C)
Precipitation	Precipitation on the day the image was acquisition (P-1) Average precipitation over 2, 3, 4 or 5 days (P-M2, P-M3, P-M4, P-M5)

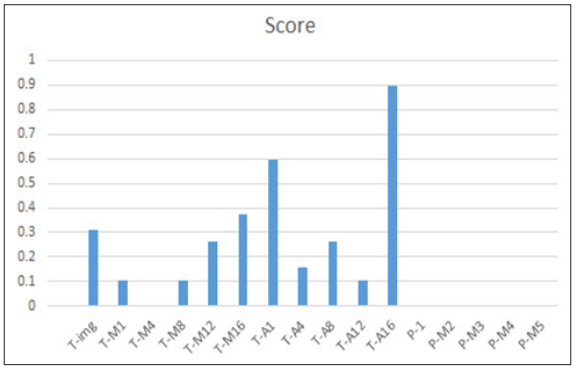

Fig. 2. Importance score

2.4 Simulation areas and data

The experimental area covers 14,400 km^2 from Odaesan, Gangwon-do, to Jecheon, Chungcheongbuk-do (Fig. 3); this area is 25 times larger than that used in La's study. Four areas covering 225 km^2 were selected to determine the differences between the regional features: a mountainous area higher than 1,000 m (Area-1), a small city with a mountainous area (Area-2), an area with relatively lower mountains (Area-3), and the suburbs of a city (Area-4; Table 3). The distribution of NDVI was calculated from the original image taken on the target date to identify the regional features (Fig. 4). There

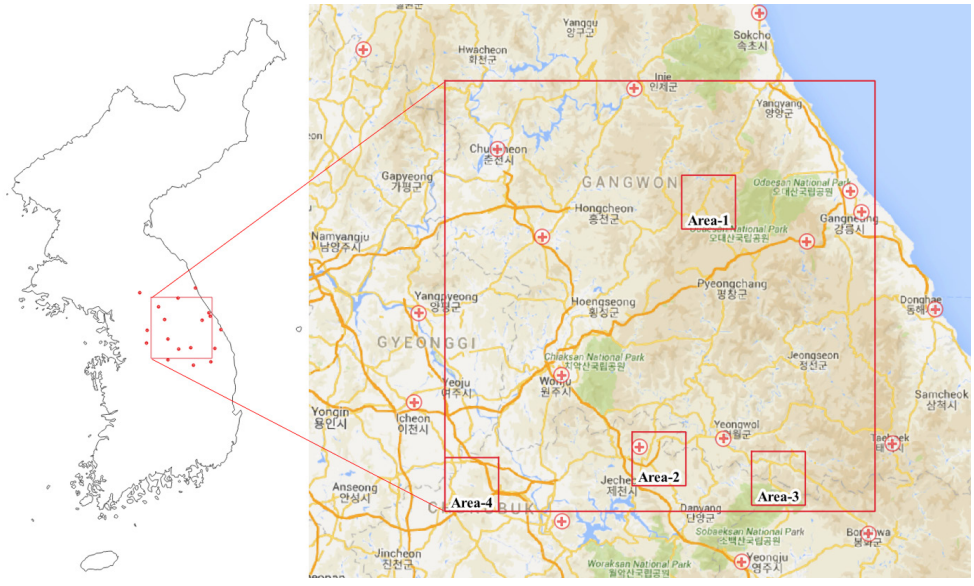

Fig. 3. Experimental area and meteorological observatory

Table 3. Location and features of the sample area

No.	Location	Features
Area-1	Nae-myeon, Hongcheon-gun, Gangwon-do	Mountainous area higher than 1,000m
Area-2	Geumseong-myeon, Jecheon-si, Chungcheongbuk-do	Small city with mountainous area
Area-3	Gimsatgat-myeon, Yeongwol-gun, Gangwon-do	Area with relatively lower mountains
Area-4	Noeun-myeon, Chungju-si, Chungcheongbuk-do	City suburbs

Table 4. Method used to apply station value

Experimental group	Application method	Application contents
La's method	Average	Apply the average as with La's method; extend the range to entire simulation area
New weather variable	Interpolation	Convert 18 observations to point shape files using spline interpolation for comparison

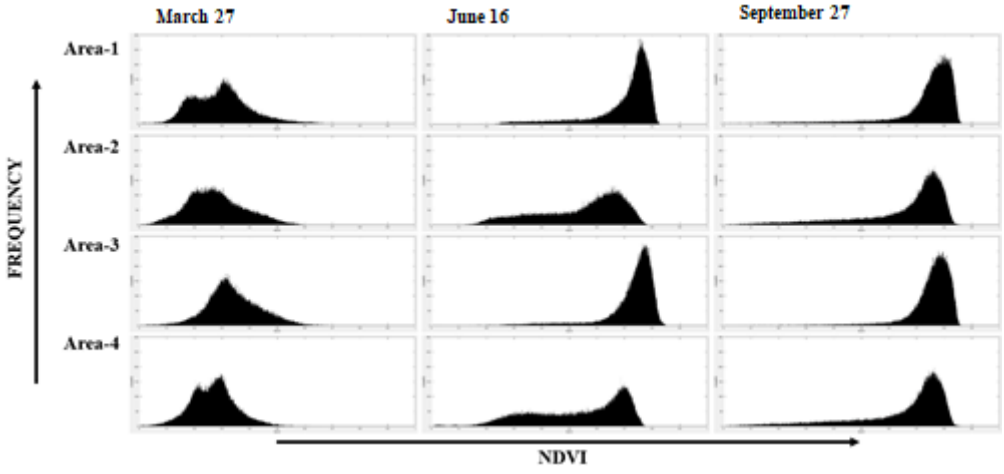

Fig. 4. NDVI distribution features by target date in each area

are 18 weather stations inside and outside the experimental areas. The study of La *et al.* (2015) used weather information from two observation stations located near the experimental area as variables. This study used the average value of 18 weather stations when reproducing La's method.

New weather variable was converted to point shape files and applied using spline interpolation (Table 4).

The set of experiments employed five years of images from LANDSAT 5 and 8 obtained in odd years between 2009 and 2017. To compare the seasonal simulations, spring, summer, and autumn data sets were used as simulation targets. However, no images were obtained in the adjacent time periods of the simulation targets, and vegetation changed rapidly during autumn targets. In addition, there is no image taken in September in other years, and, therefore, limited simulations were conducted (Table 5).

Table 5. Dates of data set acquisition(bold italic font represents the target date)

Image Product	Year	Date			
		Spring	Summer	Autumn	Winter
LANDSAT-5	2009	04-07 05-25	-	-	-
	2011	03-12 04-13	06-16	-	01-07
LANDSAT-8	2013	***03-27***	-	10-27 11-12 11-28	-
	2015	03-07 03-23 04-24 05-10 05-26	-	10-17	-
	2017	04-13 04-29	***06-16***	***09-20***	01-23 02-24 12-09 12-25

3. Simulation and Results

3.1 Simulation image

Simulations were conducted using MODIS NDVI and three solar radiation values as common variables to compare and analyze the results between the weather variables employed (Fig. 5–Experiment No.1). To reproduce La's method, the temperature, visibility, humidity, and five-day average precipitation obtained at 18 stations and the common variables were averaged and applied (Fig. 5-Experiment No. 2). A comparison was performed by applying the accumulated temperature (over 0 ℃) over 16 days obtained from 18 stations (in addition to the common variables as weather variables; Fig. 5-Experiment No.3).

The weather data used in all experiments were obtained from the weather data open portal (data.kma.go.kr), and SRTM DEM, MODIS NDVI, and LANDSAT data were downloaded from the Geological Survey of the United States (earthexplorer.usgs.gov). All grid data were unified with the same coordinate system, and they were scaled and sized through reprojection and rescaling. The NDVI was calculated from reflectance and atmospheric calibrated LANDSAT data. All variables were extracted for each pixel and subjected to multiple regression analysis (Fig. 6).

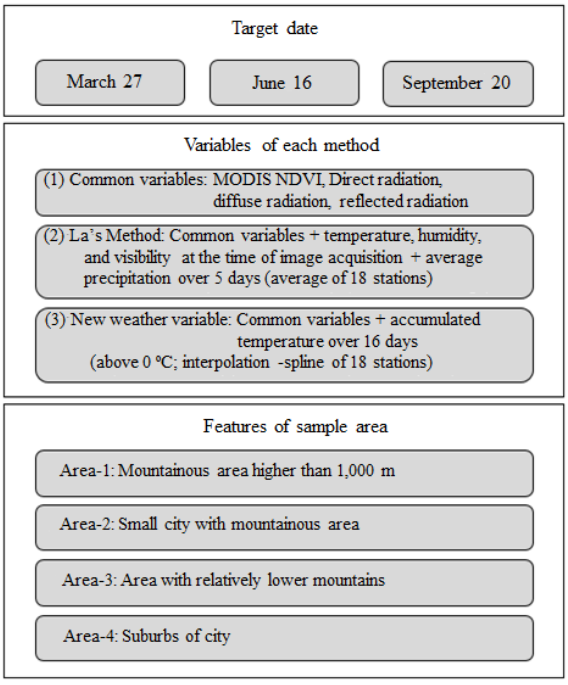

Fig. 5. Experimental composition

3.2 Simulation results

The simulations used three target dates and three variable combinations, and the regional characteristics and associated

results of the four areas were compared. In total, 36 results were generated, and the performance of each result was analyzed by calculating the coefficient of determination (R^2) and root mean-squared error (RMSE). Each of the target original image and simulated result image areas were clipped to compare the actual observation with the predicted value. R^2 and RMSE were obtained through analysis between corresponding pixels. The comparisons results are summarized by date, area, and variable used, in Table 6.

In comparison with La's method, the results of the simulations using the 16-day accumulated temperature, which is the new weather variable included in this experiment, showed an average increase and decrease of 0.0850 and 0.0249 in R^2 and RMSE, respectively, for all

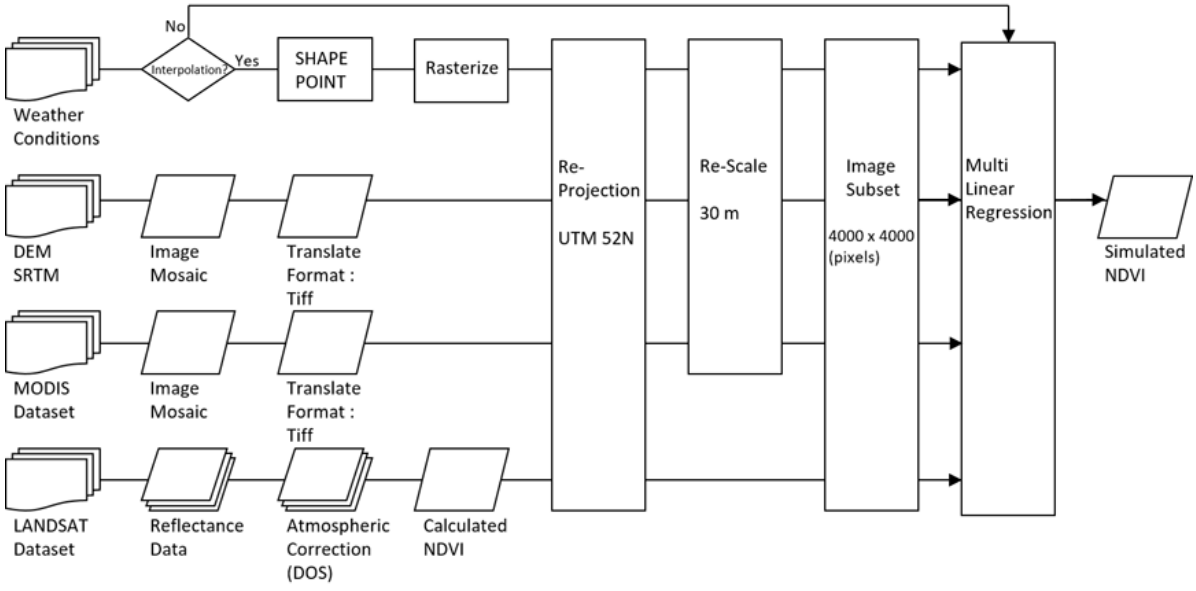

Fig. 6. Data processing flowchart

Table 6. Results by target date, regional characteristics, and variable used

Sample Area	Method No.	March 27		June 16		September 20	
		R^2	RMSE	R^2	RMSE	R^2	RMSE
Area-1	(1)	0.7806	0.0501	0.7501	0.0650	0.2607	0.2431
	(2)	0.7109	0.0522	0.6564	0.1147	0.1987	0.2365
	(3)	0.8233	0.0870	0.7576	0.1078	0.4408	0.1076
Area-2	(1)	0.8325	0.0416	0.8296	0.0731	0.5696	0.1642
	(2)	0.8335	0.0431	0.8091	0.1323	0.5552	0.1709
	(3)	0.8800	0.0527	0.8489	0.0679	0.6426	0.1177
Area-3	(1)	0.8386	0.0381	0.7589	0.0633	0.3325	0.1352
	(2)	0.8328	0.0379	0.5793	0.0725	0.2599	0.1628
	(3)	0.8663	0.0628	0.7538	0.0799	0.4795	0.0863
Area-4	(1)	0.7466	0.0480	0.8326	0.0736	0.5025	0.1625
	(2)	0.8435	0.0414	0.8211	0.1190	0.4901	0.1652
	(3)	0.7592	0.0592	0.8596	0.0709	0.4985	0.1499

cases. There was a rapid change in vegetation on September 20, and the simulation results are expected to be lower than those of the other two target dates. Nevertheless, when using the 16-day accumulated temperature, there was a significant improvement in the results. The best case for both comparisons occurred in Area-1 on September 20: the R^2 and RMSE increased and decreased by 0.2421 and 0.1289, respectively (Fig. 7), and, the average rates of increase and decrease for R^2 and RMSE were 55.95% and 35.47%, respectively.

In comparison with the simulation results using common variables alone, La's method resulted in an average R^2 and RMSE decrease and increase of 0.0370 and 0.0159, respectively. This implies that adding weather variables to the common variables at the time of image acquisition, such as when employing La's method, has a negative effect on the simulation results. The difference was found te be particularly large on June 16, R^2 and RMSE decreased and increased by 0.0763 and 0.0409, respectively.

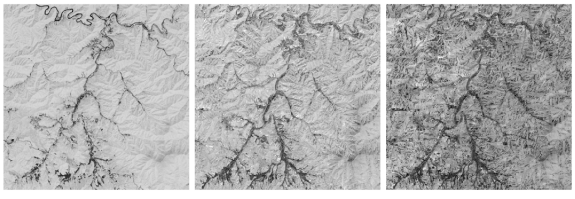

(a) (b) (c)

Fig. 7. September 20 in Area-1

(a): Original Target NDVI
(b): Employing accumulated temperature
(R^2: 0.4408, RMSE: 0.1076)
(c): La's method (R^2: 0.1987, RMSE: 0.2365)

The best simulation results for all cases and methods were obtained for Area-2 when the simulation was applied using the 16-day accumulated temperature and common variables for the target on March 27 (R^2 0.8800, RMSE 0.0527; Fig. 8).

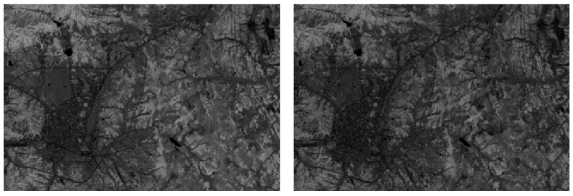

(a) (b)

Fig. 8. March 27 in Area-2

(a): Original Target NDVI
(b): Employing Accumulated Temperature
(R^2 0.8800, RMSE 0.0527)

The results for Area-2 exhibited an R^2 and RMSE that were 0.1100 higher and 0.0038 lower, respectively, than the mean of the other three regions. Additionally, the results for March 27 provided an R^2 and RMSE that were on average 0.2087 higher and 0.0714 lower, respectively, compared with the average for the other two target dates. Based on the results of the two comparisons, it was concluded that the best results were obtained on March 27 in Area-2.

To determine the differences between the regional characteristics when using the simulation method with accumulated temperature, the three target dates were averaged to compare the simulation results by region (Table 7). The results were relatively low for Area-1 and Area-3, which are mountainous regions with a large vegetation distribution, whereas those for Area-2 and Area-4 (which contain few trees and many artifacts) were relatively good. However, when calculating the rate of change when using accumulated temperature result, the R^2 result for Area-4

Table 7. Comparison of simulation result averages by region

	La's method		Using Accumulated Temperature		Rate of change	
	R^2	RMSE	R^2	RMSE	R^2	RMSE
Area-1	0.5220	0.1345	0.6739	0.1008	29.10%	-25.04%
Area-2	0.7326	0.1154	0.7905	0.0794	7.90%	-31.19%
Area-3	0.5573	0.0911	0.7000	0.0763	25.57%	-16.18%
Area-4	0.7182	0.1085	0.7058	0.0933	-1.74%	-14.00%

was found to decrease by approximately 1.7%, compared with La's method. This is due to the Area-4 result of March 27. It is the only case in which R^2 value is decreased of the entire case. Area-2 includes a small city where there is a low vegetation distribution; and the accumulated temperature in this area provide less effective results of improvement than Area-1 and Area-3.

4. Conclusion

Simulations were conducted based on La's method using common variables (MODIS NDVI, direct, diffused, and reflected radiation values) and temperature, humidity, visibility, and five-day average precipitation at the time of image acquisition. The results were inferior to those acquired using only common variables. However, when the 16-day accumulated temperature was employed, which considered vegetation growth characteristics, the simulation results were significantly improved.

The results for Area-1 (mountainous areas over 1,000 m) were the poorer than those of other areas, and the results for September 20 were the poorest of all the target dates. Forest distribution is difficult to simulate and it was difficult to conduct simulations because images were lacking from adjacent periods. However, the most effective improvement in the simulation method using the 16-day accumulated temperature (compared with La's method) was observed in Area-1 for September 20, which is considered to be the season with the worst conditions. The use of the 16-day accumulated temperature, which is a variable that reflects vegetation growth characteristics, improved the performance results, and was also found to be more effective in forested areas, where trees were dense, and in extreme situations, where reference data were lacking.

When simulations are conducted over large areas, a large number of station data related to the simulation area are required for use as variables. However, additional interpolation experiments are required, and it is necessary to conduct further experiments using the geographical characteristics of stations, such as differences in altitude and the surrounding topography. In this experiment, 16-day accumulated temperature was used to confirm the availability of variables with growth characteristics. However, other variables such as ground temperature, ground humidity, and geology also directly affect vegetation. Common weather observation data for North and South Korea, including humidity, precipitation, and visibility, can be employed in addition to temperature. If the relationship between these data and vegetation growth is determined, it may be possible to select additional variables and conduct detailed simulations by employing a multi-faceted approach to vegetation growth characteristics.

References

Arnon, D.I., Allen, M.B., and Whatley, F.R. (1956), Photosynthesis by isolated chloroplasts IV. General concept and comparison of three photochemical reactions, *Biochimica et Biophysica Acta-General Subjects*, 20, pp.449-461.

Boussetta, S., Balsamo, G., Beljaars, A., Kral, T., and Jarlan, L. (2013), Impact of a satellite-derived leaf area index monthly climatology in a global numerical weather prediction model, *International journal of remote sensing*, 34(9-10), pp.3520-3542.

Breiman, L. (2001), Random forests, Machine learning, 45(1), pp.5-32.

Corenblit, D. and Steiger, J. (2009), Vegetation as a major conductor of geomorphic changes on the Earth surface: toward evolutionary geomorphology, *Earth Surface Processes and Landforms*, 34(6), pp.891-896.

Fenner, M. (1998), The phenology of growth and reproduction in plants, *Perspectives in Plant Ecology, Evolution and Systematics*, 1(1), pp.78-91.

Frey, H. and Paul, F. (2012), On the suitability of the SRTM DEM and ASTER GDEM for the compilation of topographic parameters in glacier inventories, *International Journal of Applied Earth Observation and Geoinformation*, 18, pp.480-490.

Gao, F., Masek, J., Schwaller, M., and Hall, F. (2006), On the blending of the Landsat and MODIS surface reflectance: Predicting daily Landsat surface reflectance, *IEEE Transactions on Geoscience and Remote sensing*, 44(8), pp.2207-2218.

Gates, D.M. (2012). *Biophysical Ecology*, Courier Corporation.

Hänninen, H. and Tanino, K. (2011), Tree seasonality in a warming climate, *Trends in plant science*, 16(8), pp.412-416.

Hirt, C., Filmer, M.S., and Featherstone, W. E. (2010), Comparison and validation of the recent freely available ASTER-GDEM ver1, SRTM ver4. 1 and GEODATA DEM-9S ver3 digital elevation models over Australia, *Australian Journal of Earth Sciences*, 57(3), pp.337-347.

Jensen, J.R. (2009), *Remote Sensing of the Environment: An Earth Resource Perspective 2/e*, Pearson Education India.

Kim, J.S., Jeong, M.I., Han, S.W., Jang, H.K., and Jung, H.H. (2014), Analysis of Accumulated Temperature According to Sprouting of 3 Garden Woody Plants, *Journal of People Plants and Environment*, 17(6), pp.471-475. (in Korean with English abstract)

Kim, H.J., Seo, D.K., Eo, Y.D., Jeon, M.C., and Park, W.Y. (2019), Multi-temporal Nonlinear Regression Method for Landsat Image Simulation, *KSCE Journal of Civil Engineering*, 23(2), pp.777-787.

Kumar, L., Skidmore, A.K., and Knowles, E. (1997), Modelling topographic variation in solar radiation in a GIS environment, *International Journal of Geographical Information Science*, 11(5), pp.475-497.

La, H.P., Eo, Y.D., Lee, S.B., Park, W.Y., and Koo, J.H. (2015), Image simulation from multitemporal landsat images, *GIScience and Remote Sensing*, 52(5), pp.586-608.

Lanorte, A., Lasaponara, R., Lovallo, M., and Telesca, L. (2014), Fisher–Shannon information plane analysis of SPOT/VEGETATION Normalized Difference Vegetation Index (NDVI) time series to characterize vegetation recovery after fire disturbance, *International Journal of Applied Earth Observation and Geoinformation*, 26, pp.441-446.

Lee, M.H., Lee, S.B., Eo, Y.D., Kim, S.W., Woo, J.H., and Han, S.H. (2017), A comparative study on generating simulated Landsat NDVI images using data fusion and regression method—the case of the Korean Peninsula, *Environmental monitoring and assessment*, 189(7), 333p.

Li, X. and Yeh, A.G. (2004), Multitemporal SAR images for monitoring cultivation systems using case-based reasoning, *Remote Sensing of Environment*, 90(4), pp.524-534.

McMaster, G.S. and Wilhelm, W. (1997), Growing degree-days: one equation, two interpretations, *Agricultural and Forest Meteorology*, 87, pp.291-300.

Monteith, J.L. (1981). Climatic variation and the growth of crops, *Quarterly Journal of the Royal Meteorological Society*, 107(454), pp.749-774.

Pettorelli, N., Vik, J.O., Mysterud, A., Gaillard, J.M., Tucker, C.J., and Stenseth, N.C. (2005), Using the satellite-derived NDVI to assess ecological responses to environmental change, *Trends in ecology and evolution*, 20(9), pp.503-510.

Robinson, N.P., Allred, B.W., Jones, M.O., Moreno, A., Kimball, J.S., Naugle, D.E., and Richardson, A.D. (2017), A dynamic Landsat derived normalized difference vegetation index (NDVI) product for the conterminous United States, *Remote Sensing*, 9(8), 863p.

Seo, D.K., Kim, Y.H., Eo, Y.D., Park, W.Y., and Park, H.C. (2017), Generation of radiometric, phenological normalized image based on random forest regression for change detection, *Remote Sensing*, 9(11), 1163p.